Increased microglial activation in patients with Parkinson disease using [^{18}F]-DPA714 TSPO PET imaging

Sonia Lavisse, Sébastien Goutal, Catriona Wimberley, Mattéo Tonietto, Michel Bottlaender, Philippe Gervais, Bertrand Kuhnast, Marie-Anne Peyronneau, Olivier Barret, Julien Lagarde, et al.

TITLE PAGE

Increased microglial activation in patients with Parkinson disease using [^{18}F]-DPA714 TSPO PET imaging

AUTHORS

Sonia Lavisse[a,*], PhD, Sébastien Goutal[a], Catriona Wimberley[b,1], PhD, Mattéo Tonietto[b], PhD, Michel Bottlaender[b,c], MD, PhD, Philippe Gervais[b], Bertrand Kuhnast[b], PhD, Marie-Anne Peyronneau[b], PhD, Olivier Barret[a], PhD, Julien Lagarde[b,d,e], MD, Marie Sarazin[b,d,e], MD, PhD, Philippe Hantraye[a], PhD, Claire Thiriez[f,2],MD, Philippe Remy[a,f,g], MD, PhD.

Email addresses :
sonia.lavisse@cea.fr; sebastien.goutal@cea.fr; cwimberl@ed.ac.uk; matteo.tonietto@cea.fr; michel.bottlaender@cea.fr; philippe.gervais@cea.fr; bertrand.kuhnast@cea.fr; marie-anne.peyronneau@cea.fr; olivier.barret@cea.fr; j.lagarde@ghu-paris.fr; m.sarazin@ghu-paris.fr; philippe.hantraye@cea.fr; claire_thiriez@yahoo.com ; neuro-philippe.remy@aphp.fr

INSTITUTIONAL ADDRESSES

[a] Université Paris-Saclay, CEA, CNRS, MIRCen, Laboratoire des Maladies Neurodégénératives, 92265, Fontenay-aux-Roses, France
[b] Université Paris-Saclay, CEA, CNRS, Inserm, BioMaps, Service Hospitalier Frédéric Joliot, 4, place du général Leclerc, Orsay, 91401, France
[c] Université Paris-Saclay, UNIACT, Neurospin, CEA, 91191 Gif-sur-Yvette
[d] Department of Neurology of Memory and Language, GHU Paris Psychiatrie & Neurosciences, Sainte-Anne hospital, Paris, 75014, France
[e] Université de Paris, F-75006 Paris.
[f] Centre Expert Parkinson, Neurologie, CHU Henri Mondor, AP-HP, 51 avenue du Maréchal de Lattre de Tassigny, Créteil, France
[g] IMRB, INSERM, Université Paris Est Créteil and NeurATRIS, France

Present address:
[1] Edinburgh Imaging facility QMRI, The University of Edinburgh, Edinburgh, United Kingdom
[2]Service de neurologie et Centre Expert Parkinson, CHU de Caen, France

Corresponding author : Sonia Lavisse (sonia.lavisse@cea.fr)

18 route du Panorama - 92260 Fontenay-aux-Roses
Phone number : 33-1-46548409

Declarations of interest: none

ABSTRACT

Introduction

Increasing evidence suggests that neuroinflammation is active in Parkinson disease (PD) and contribute to neurodegeneration. This process can be studied *in vivo* with PET and radioligands targeting TSPO, upregulated in activated microglia. Initial PET studies investigating microglial activation in PD with the [^{11}C]-PK11195 have provided inconclusive results. Here we assess the presence and distribution of neuroinflammatory response in PD patients using [^{18}F]-DPA714 and to correlate imaging biomarkers to dopamine transporter imaging and clinical status.

Methods

PD patients (n=24, Hoehn and Yahr I-III) and 28 healthy controls were scanned with [^{18}F]-DPA714 and [^{11}C]-PE2I and analyzed. They were all genotyped for TSPO polymorphism. Regional binding parameters were estimated (reference Logan graphical approach with supervised cluster analysis). Impact of TSPO genotype was analyzed using Wilcoxon signed-rank test. Differences between groups were investigated using a two-way ANOVA and Tukey *post hoc* tests.

Results

PD patients showed significantly higher [^{18}F]-DPA714 binding compared to healthy controls bilaterally in the midbrain ($p < 0.001$), the frontal cortex ($p = 0.001$), and the putamen contralateral to the more clinically affected hemibody ($p = 0.038$). Microglial activation in these regions did not correlate with the severity of motor symptoms, disease duration nor putaminal [^{11}C]-PE2I uptake. However, there was a trend toward a correlation between cortical TSPO binding and disease duration ($p = 0.015$ uncorrected, $p = 0.07$ after Bonferroni correction).

Conclusion

[^{18}F]-DPA714 binding confirmed that there is a specific topographic pattern of microglial activation in the nigro-striatal pathway and the frontal cortex of PD patients.

Trial registration: Trial registration: INFLAPARK, NCT02319382. Registered 18 December, 2014- Retrospectively registered, https://clinicaltrials.gov/ct2/show/NCT02319382

Key words : Microglia; TSPO; [^{18}F]-DPA714; PET; Parkinson disease, neuroinflammation

BACKGROUND

In Parkinson disease (PD), neuroinflammation is thought to play an important role in the progression of the neurodegeneration process [1-3]. Studies have described the presence of reactive microglia in *postmortem* brain samples of PD patients [1]. Specifically, major histocompatibility complex class II immunoreactive microglia was identified in the Substantia nigra (SN) and the striatum [4]. Located in the vicinity of the remaining nigral dopaminergic (DA) neurons, these microglial cells displayed morphologies characteristic of activated and phagocytic cells, similar to those seen in aging [1, 5]. Studies of *postmortem* human brains and animal models of parkinsonism further strongly suggest an involvement of neuroinflammation in the pathological process. However, several questions remain unresolved, such as the topography of neuroinflammation *in vivo* compared to *postmortem*, the relationship between the severity of the disease and the intensity of neuroinflammatory response in the brain and the time sequence of this process as primary or secondary marker of the disease [6].

To investigate these questions in PD patients, positon emission tomography (PET) imaging studies have widely relied on a radioligand, the [^{11}C]-PK11195, that binds to the translocator protein (TSPO). This protein is expressed at low levels in healthy brains but is markedly upregulated on activated microglia and astrocytes in the presence of inflammation in several acute and degenerative disorders [7]. Studies with [^{11}C]-PK11195 have led to considerable advancement in understanding the pathophysiological implication of microglial activation in several neurodegenerative diseases. In PD patients, early PET studies conducted by Gerard *et al*. and Ouchi *et al*. revealed an increase in [^{11}C]-PK11195 binding in nigrostriatal structures (basal ganglia and midbrain) [8, 9]. However, the use of this radioligand is limited by low brain permeability, a high nonspecific binding (to brain and to plasma proteins, monocytes and platelets) and a relatively short half-life of carbon-11 (see

reviews [10, 11]). These restrictions have prompted over the last twenty years the development of second-generation TSPO radioligands with higher signal to noise ratio in an attempt to improve quality of TSPO imaging. Owen *et al.* reported that these new TSPO ligands however are sensitive to the single-nucleotide polymorphism, rs6971, located in the TSPO gene in humans that accounts for variable affinity patterns [15]. Therefore, PET scans using second-generation TSPO ligands should be analyzed only after considering the rs6971 polymorphism of each subject. Some of these TSPO ligands such as [^{18}F]-FEPPA, [^{11}C]-PBR28, [^{11}C]-DPA713 have been used to investigate microglial activation in PD [10, 12, 14, 16].

Among second-generation TSPO radiotracers, [^{18}F]-DPA714 has shown high affinity for TSPO, a high brain penetration and favorable pharmacokinetics [17] with the Logan graphical analysis. Its quantification has been validated in healthy volunteers using first the two-tissue compartment model with arterial input function and second, and the supervised cluster analysis (SVCA) [18]. In the present study, we investigated whether TSPO imaging with [^{18}F]-DPA714 could be used as a potential and sensitive biomarker of microglial activation in PD and how it compares with previous studies using other second-generation radioligands.

By accounting for the TSPO polymorphism, we studied microglial activation in healthy controls (HC) and in PD patients at different disease stages and investigated the microglial activation along with presynaptic dopamine transporter (DAT) density imaging using the [^{11}C]-PE2I radioligand. We sought to measure the regional brain distribution of activated microglia especially in the midbrain and various dopaminergic pathways of PD patients and to determine in these regions whether neuroinflammation correlates with disease severity measured through clinical motor scores and presynaptic DAT abnormalities.

METHODS

Subjects

Twenty-four patients meeting UK Brain Bank criteria for the diagnosis of idiopathic PD (63.5±9.8 years; 8 women, 16 men; NCT02319382) and 28 age-matched healthy controls (HC) (57.4 ±13.2 years; 15 women, 13 men, NCT02319382, NCT01775696) were enrolled in this study. All participants provided written informed consent. The protocols were approved by the French Medical Bioethics Committee and were in accordance with French legislation and the Declaration of Helsinki 1975 (revised in 1983). Patients were recruited at the Henri Mondor hospital and controls were recruited by in-house advertisements.

None of the subjects had any evidence of severe cognitive decline or history of hallucinations. Exclusion criteria for all participants included: (1) history of head injury, psychiatric or other neurological disease, except PD for the patients; (2) alcohol or drug abuse; (3) contra-indications for MRI scanning; (4) use of any drug interacting with DAT or TSPO binding (e.g., benzodiazepines or derivatives that are not specific to central benzodiazepine binding site) or TSPO expression (nonsteroidal anti-inflammatory drugs more than 50 days within the last year or more than 7 days within the last month); and (5) clinically significant lesion on brain MRI.

The selection of PD patients purposely included patients at different stages: early drug-naïve patients (n=9), patients with longer disease duration (>36 mo, < 5 years) without motor fluctuations (n=9) and more advanced patients having motor fluctuations and disease for at least 5 years (n=6). Disease duration was calculated from the first clinical diagnosis of PD.

All participants underwent PET and anatomical MRI scans on the same day. Medications of PD patients were withdrawn about 15 hours before scanning (last dose was taken the night before; two nights before for extended release dopamine agonists). Clinical evaluations were performed using the MDS-UPDRS motor score in on-state during the hospital visit a few days

or up to 6 weeks before the PET sessions. MDS-UPDRS in off-state and quality of life with the PDQ-39 were evaluated by the same neurologist on the day of PET imaging.

Genomic DNA from blood samples was used to genotype the rs6971 polymorphism of the TSPO gene to stratify all subjects into high (HAB), mixed (MAB) and low (LAB) affinity binders.

Imaging protocol

MR images were acquired to ensure the absence of brain lesion and for co-registration with the PET images to anatomically delineate the Volumes-of-Interest (VOIs). T1-weighted imaging was performed using a turbo spin echo sequence on a 1.5 Tesla Philips Achieva system (Best, The Netherlands) or a MPRAGE sequence on a 3.0 Tesla TRIO MRI scanner (Siemens Healthcare, Germany).

[^{18}F]-DPA714 was prepared according to standard conditions [19] and [^{11}C]-PE2I synthesis was performed as previously reported [20]. The short half-life of 11-Carbone (20 minute) allowed both PET scans to be performed in a single day for each participant. All exams were acquired on a High Resolution Research Tomograph (HRRT; CTI/Siemens Molecular Imaging) allowing imaging of small volume structures. A custom-fitted mask was applied for each subject to minimize head movements. PET dynamic acquisitions lasted up to 60 minutes after injection of [^{11}C]-PE2I (mean 293.4±78 MBq) and [^{18}F]-DPA714 (mean 207.9±42.7 MBq) was injected 3 hours later (90-min acquisitions).

Image processing

The partial volume effect was reduced by directly incorporating resolution modelling inside the iterative algorithm during reconstruction of PET images [21].

The TSPO protein has a widespread distribution and consequently, no single region free of this target can be identified as a reference for non-specific ligand binding. Supervised cluster analysis (SVCA), previously described and validated with [^{18}F]-DPA714 images [18], was

therefore used to extract a distributed cluster of voxels with a time activity curve that represents the reference curve of a normal population.

A VOI-based approach was performed using an automatic segmentation of grey matter on individual MRI using the VBM package implemented in SPM8 (Statistical Parametric Mapping, Wellcome Trust Centre for Neuroimaging) and the Volbrain pipeline for sub-cortical regions [22]. The automated anatomical labelling atlas (AAL), previously applied in PD patients [23], was deformed to each MRI and applied after co-registration to the PET dynamic data in order to measure [^{11}C]-PE2I and [^{18}F]-DPA-714 uptakes in 90 anatomical regions. These VOIs were defined in both hemispheres and were then regionally pooled into larger anatomical VOIs. We defined the following VOIs: caudate (7.13±0.96 mL), putamen (7.80±0.86 mL), globus pallidus (2.39±0.33 mL), cerebellum (49.81±5.94 mL), thalamus (10.47±0.97), amygdala (1.59±0.22 mL) and gray matter of frontal, temporal, parietal and occipital cortices (93.72±12.89, 106.46±13.60, 35.36±5.02 and 58.32±8.43 mL, respectively). 'Whole cortical' [^{18}F]-DPA714 binding was considered as the average of values in the cortical regions. Midbrain region was manually delineated by an experienced neurologist (PR) on individual MRI to include the whole substantia nigra (2.88±0.60 mL) (Figure1A). In patients, more (+) and less (-) sides for sub-cortical regions were defined as contralateral to the clinically more and less affected sides based on MDS-UPDRS measurements. In HC, we found no significant difference in microglial activation between the right and left sides for all the regions explored. Therefore, measurements of both hemispheres were averaged.

The Logan's Reference Tissue Model (Pmod® software) used for [^{18}F]-DPA714 analysis, yielded regional non-displaceable binding potential (BP_{ND}) estimates in each VOI [24]**.** The Simplified Reference Tissue Model with cerebellum as reference input function was used for [^{11}C]-PE2I to calculate the DAT binding in striatal structures (BP_{ND}) [25].

Statistics

All data are presented as mean ± SD. Statistical analysis was performed using the R project software. Demographic and clinical measures were compared using a two-way ANOVA with disease (PD and controls) and TSPO genotype as factors. The impact of TSPO genotype in participants was analyzed using Wilcoxon signed-rank test. Differences in [^{18}F]-DPA714 BP_{ND} values between HC and patients and between patients at the three different disease stages were analyzed in all regions, using a two-way ANOVA and Tukey *post hoc* tests, with genotype and disease stage as factors. To remove the effect of affinity on clinical-PET correlations, individual BP_{ND} estimates in each cortical region were normalized by the mean BP_{ND} of their corresponding affinity group (HAB or MAB) to correlate normalized BP_{ND} with disease duration. All correlations were analyzed using the Pearson correlation test (Pearson correlation coefficient *r*). The Hampel method and the Grubbs test were used to reveal any clinical data outlier and a Bonferroni correction was applied for multiple comparisons. Statistical significance was set to $p < 0.05$.

RESULTS

Subjects

One patient was excluded from the analyses because he could not complete the [^{18}F]-DPA714 scan. Two HC were excluded from the study due to frontal lesion on the brain MRI and essential tremor. Therefore, 23 PD patients and 26 HC were analyzed. Demographic and clinical data of patients are shown in Table 1. The diagnosis of PD was supported by quantitative evaluation of DAT binding using [^{11}C]-PE2I PET. BP_{ND} values in the putamen were significantly lower in patients (BP_{ND}= 2.65 ± 1.27) than in controls (BP_{ND}=8.7 ± 3.33, $p < 0.001$). In all PD patients, the lowest putaminal DAT binding was contralateral to the clinically more affected side.

Genomic analysis in HC and patients revealed 13 and 7 HABs, 12 and 13 MABs and 1 and 3 LABs, respectively. Analyses performed on LABs could not accurately quantify the [^{18}F]-DPA714 binding nor provide accurate BP_{ND} values unlike in MAB and HAB subjects. Therefore, LABs were excluded from further statistical analyses and interpretation. No difference in disease duration, disease severity or DAT binding was found between the HAB and the MAB groups and no statistical outliers in the clinical data were observed.

TSPO binding in PD patients

Factorial ANOVAs revealed that the [^{18}F]-DPA714 binding was significantly higher in the midbrain of PD patients compared to HC (Figure 2). This increase was found both in the predominantly affected side ($p < 0.001$ in midbrain+; +68.8% in HABs and +58.1% in MABs) and the less affected side ($p < 0.001$ in midbrain-, +12.6% in HABs and +44.1% in MABs). In PD patients, [^{18}F]-DPA714 binding was significantly higher in midbrain+ than in the midbrain- region (p =0.045; +49.9% and +9.7% in HABs and MABs, respectively, Figure 1B).

In addition, microglial activation was significantly higher in patients than in HC in the Putamen+ (p = 0.038; 27.3% and +68.9% in HABs and MABs, respectively). There was an increase of microglial activity in Putamen- region which did not reach statistical significance (p = 0.08; +21.6% and +66.0% in HABs and MABs).

In the frontal cortex, TSPO binding was significantly higher in patients than in HC with an average increase of +38.2 % (p = 0.001, HAB +34.7%, MAB +41.6%, Table 2). In the other cortical regions, there was no significant increase of TSPO expression in the PD patients (Table 2).

Differences in regional [^{18}F]-DPA714 binding between patients and healthy controls were also investigated with a voxel-based analysis using SPM. Voxel clusters extracted with this

method were found in similar regions than those displaying significant [^{18}F]-DPA714 increase in the ROI-based approach (Supplementary Figure1).

Correlations

There was no correlation between [^{18}F]-DPA714 binding and age in controls and in patients across regions. In patients, we found no significant correlation between putaminal [^{11}C]-PE2I DAT binding and [^{18}F]-DPA714 binding in the midbrain and the striatum. In addition, there was no correlation between disease duration or MDS-UPDRS motor scores and [^{18}F]-DPA714 BP_{ND} in the midbrain, putaminal and frontal regions. Nevertheless, [^{18}F]-DPA714 binding in the whole cortex was correlated with disease duration (Pearson, $r = 0.55$, $p = 0.015$ which did not stand up to Bonferroni correction: $p = 0.071$, supplementary Figure 2).

TSPO polymorphism effect

Overall, there was a significant main effect of TSPO genotype in HC ($p < 0.001$) and in patients ($p = 0.007$) with significantly higher [^{18}F]-DPA714 BP_{ND} estimates in HABs compared to MABs (+21.8 ±10.0% in HC and +9.2 ±16.7% in patients). Regions that had the greatest percent differences included the thalamus, putamen and globus pallidum (Table 2).

DISCUSSION

There is a consensus on the probable role of neuroinflammation in the degenerative process of PD, which might therefore be considered as a potential therapeutic target for neuroprotective studies. This study is the first use of [^{18}F]-DPA714 to compare microglial activation in Parkinsonian patients and HC, all genotyped for TSPO polymorphism. Our analyses demonstrated significantly higher [^{18}F]-DPA714 BP_{ND} in the midbrain, putaminal and frontal cortical regions in patients compared to HC. The ROI-based analysis was further confirmed

by the voxel-based approach. This binding was not correlated with markers of disease progression, such as disease duration, MDS-UPDRS motor scores or DAT binding. We found a trend for a positive correlation between [^{18}F]-DPA714 binding in the whole cortex and disease duration, suggesting an accumulation of inflammation in cortical areas over years in PD.

Microglial activation in the midbrain

We found increased TSPO binding bilaterally in the midbrain/SN of PD patients. This is in line with five previous studies using either [^{11}C]-PK11195 [9, 13, 26, 27] or the more recent [^{11}C]-DPA713 [16]. Midbrain/SN was not investigated in two studies [12, 28]. Conversely, no significant increase of TSPO was found in the midbrain/SN in three studies using either [^{11}C]-PK11195 [8, 29] or the second-generation ligand [^{11}C]-PBR28 [14]. Altogether, midbrain/SN activation can be found in most studies considering that region and using either [^{11}C]-PK11195 or second-generation – more specific – TSPO radioligands. These results obtained *in vivo* confirm the role of microglial activation in the pathophysiology of PD, in agreement with postmortem studies showing the presence of microglia activation nearby the dopaminergic neurons degeneration in the SN pars compacta [3, 4].

In our PD patients, the presence of activated microglia was bilateral in the midbrain but was significantly more pronounced in the side more affected by the disease process. This suggests that inflammation accumulates with disease progression, independently of the number of remaining dopaminergic neurons. In line with most previous studies, we found no correlation between disease duration or severity and TSPO binding in the midbrain regions. Conversely, Ouchi *et al.* [30] found a significant relationship between midbrain TSPO binding and two markers of disease severity: UPDRS motor score and DAT binding in the putamen, suggesting that TSPO binding increases with disease severity. However, this analysis was performed in a small group of patients at an early stage of the disease and was not reproduced

thereafter, even in the present study with a larger number of patients at different stages of the disease and using identical disease severity markers. This lack of correlation could be explained on one hand by the fact that microglial activation may be present long before symptoms onset of PD and that there might be a threshold of microglial activity necessary for cell death to occur. On the other hand, microglial activity and phenotype might fluctuate over time independently of clinical progression of the disease, which would be more related to the progressive dysfunction of the dopaminergic system and counterbalancing compensatory mechanisms [31].

Microglial activation in the striatum

Interestingly, microglial activation was present in the more affected putamen and did not reach statistical significance ($p = 0.08$) in the less affected putamen. This asymmetry reproduces the asymmetry of microglial activation observed at the midbrain/SN level described above to a lesser extent. Therefore, it might be related to the degenerative process involving the SN neurons projecting mainly to the putamen. Across the literature, striatal increase of TSPO binding using PET imaging has been inconsistently reported. Gerhard *et al*. [8] and Terada *et al.* [16] found an increase in TSPO binding in the whole striatum of their patients who were at different stages of the disease. Iannacone *et al.* [13] and Kang *et al.* [26] found an increase of TSPO binding in the putamen only, whereas Edison *et al.* [28] found a striatal increase only in demented PD patients. In addition, increased TSPO binding has also been reported in the striatum of patients with multisystem atrophy and progressive supranuclear palsy [8, 32]. These latter examples suggest that direct neuropathological lesions of the putamen definitively contribute to inflammatory response in the striatum. However, the amplitude of [^{18}F]-DPA714 increase being more important in the midbrain than in the putamen of our non-demented patients, our hypothesis is that the latter is secondary to the former and might therefore be considered as a spreading of the disease process along the

nigro-striatal dopaminergic system. This is in line with a report from Stokholm et al., [33] showing increased microglial activation in the midbrain but not the putamen of subjects with REM-sleep behavior disorders exhibiting a premanifest decrease of dopamine functions.

Microglial activation in the cortex

We also found microglial activation in the frontal region in PD relative to HC. In previous PET studies, Iannacone *et al*. [13] and Edison *et al.* [28] found a marked [^{11}C]-PK11195 increase (respectively +50% and +30%) of frontal TSPO binding which however did not reach statistical significance, in early PD patients. Terada and colleagues found a significant increase of [^{11}C]-DPA713 binding in the frontal cortex of more advanced patients [16]. Again, none of these studies, including the present one, could report a relationship between disease severity or [^{11}C]-PE2I striatal binding and the amount of frontal inflammation markers. However, this does not discard a trend to a progressive cortical inflammation process occurring in PD. Indeed, Terada *et al.*, found an increase of TSPO binding in the frontal cortex of PD patients that were rescanned one year after the first examination [28]. Moreover, in our patients, there is a trend for a correlation between disease duration and the binding of [^{18}F]-DPA714 in the whole cortical mantle ($r = 0.55$, $p = 0.071$ after Bonferroni correction), suggesting a subtle inflammatory spreading process to the whole cortex over years, as reported by Gerhard and colleagues using [^{11}C]-PK11195 [8]. Moreover, other authors have reported significantly increased cortical TSPO binding in patients with PD-dementia [28] and diffuse Lewy body disease [13]. Our interpretation of these data is that cortical markers of inflammation might be present early in the frontal cortex of PD patients and spread to the whole cortical mantle over time. It is unclear whether such progression might be related to Lewy bodies spreading and to the risk of developing dementia, as it has been shown in Alzheimer disease [34], but this hypothesis might be explored in future studies.

Methodological issues and sensitivity to TSPO polymorphism

There have been eleven previous PET studies investigating inflammation in PD and results have been heterogeneous. These discrepancies can be attributed to several factors such as the various stages of the disease in the patients, the small cohorts of patients, the resolution of the scanners employed or the use of different radioligands across studies. And future studies using [^{18}F]-DPA714 in a larger and different cohort of PD patients will be necessary to confirm our results. Moreover, unlike with [^{11}C]-PK11195, the rs6971 polymorphism has been observed with several second-generation TSPO tracers both in controls and in PD patients [12, 14] and the lack of TSPO genotyping had likely an impact on the results of former PET studies in PD [16]. Our data confirm the marked impact of this polymorphism on the binding of the [^{18}F]-DPA714 radioligand to its target, both in HC and in PD patients, that consequently affects PET images and interpretation. This has already been observed with other second-generation TSPO tracers in HC and PD patients [12, 14]. It is therefore mandatory to stratify participants into matched affinity groups to compare patients to controls but this implies the genotyping of all participants and probably the exclusion of LAB subjects whose TSPO PET binding is not quantifiable. In our study, 13% of PD patients were LABs and therefore excluded. In a representative caucasian population, LABs represent 5-10% of the subjects [15] which induces a minimal loss of representativity of the population if LABs are excluded.

CONCLUSION

Using the [^{18}F]-DPA714 second-generation TSPO radioligand, we found a significant neuroinflammatory response in the midbrain, the putamen and the frontal cortex of PD patients. It seems that inflammation progressively involves the whole cortical mantle over

302 years in PD, and might reveal spreading of pathological process. [^{18}F]-DPA714 might be used
303 to explore the impact of specific anti-inflammatory drugs in this disease.

REFERENCES

[1] E.C. Hirsch, S. Vyas, S. Hunot, Neuroinflammation in Parkinson's disease, Parkinsonism & related disorders 18 Suppl 1 (2012) S210-2.

[2] S. Przedborski, Inflammation and Parkinson's disease pathogenesis, Movement disorders : official journal of the Movement Disorder Society 25 Suppl 1 (2010) S55-7.

[3] K. Kaur, J.S. Gill, P.K. Bansal, R. Deshmukh, Neuroinflammation - A major cause for striatal dopaminergic degeneration in Parkinson's disease, J Neurol Sci 381 (2017) 308-314.

[4] K. Imamura, N. Hishikawa, M. Sawada, T. Nagatsu, M. Yoshida, Y. Hashizume, Distribution of major histocompatibility complex class II-positive microglia and cytokine profile of Parkinson's disease brains, Acta Neuropathol 106(6) (2003) 518-26.

[5] P.L. McGeer, E.G. McGeer, Inflammation and the degenerative diseases of aging, Ann N Y Acad Sci 1035 (2004) 104-16.

[6] M.G. Tansey, M.S. Goldberg, Neuroinflammation in Parkinson's disease: its role in neuronal death and implications for therapeutic intervention, Neurobiology of disease 37(3) (2010) 510-8.

[7] M.K. Chen, T.R. Guilarte, Translocator protein 18 kDa (TSPO): molecular sensor of brain injury and repair, Pharmacology & therapeutics 118(1) (2008) 1-17.

[8] A. Gerhard, N. Pavese, G. Hotton, F. Turkheimer, M. Es, A. Hammers, K. Eggert, W. Oertel, R.B. Banati, D.J. Brooks, In vivo imaging of microglial activation with [11C](R)-PK11195 PET in idiopathic Parkinson's disease, Neurobiology of disease 21(2) (2006) 404-12.

[9] Y. Ouchi, E. Yoshikawa, Y. Sekine, M. Futatsubashi, T. Kanno, T. Ogusu, T. Torizuka, Microglial activation and dopamine terminal loss in early Parkinson's disease, Annals of neurology 57(2) (2005) 168-75.

[10] L. Best, C. Ghadery, N. Pavese, Y.F. Tai, A.P. Strafella, New and Old TSPO PET Radioligands for Imaging Brain Microglial Activation in Neurodegenerative Disease, Current neurology and neuroscience reports 19(5) (2019) 24.

[11] A.C. Dupont, B. Largeau, M.J. Santiago Ribeiro, D. Guilloteau, C. Tronel, N. Arlicot, Translocator Protein-18 kDa (TSPO) Positron Emission Tomography (PET) Imaging and Its Clinical Impact in Neurodegenerative Diseases, International journal of molecular sciences 18(4) (2017).

[12] C. Ghadery, Y. Koshimori, S. Coakeley, M. Harris, P. Rusjan, J. Kim, S. Houle, A.P. Strafella, Microglial activation in Parkinson's disease using [(18)F]-FEPPA, Journal of neuroinflammation 14(1) (2017) 8.

[13] S. Iannaccone, C. Cerami, M. Alessio, V. Garibotto, A. Panzacchi, S. Olivieri, G. Gelsomino, R.M. Moresco, D. Perani, In vivo microglia activation in very early dementia with Lewy bodies, comparison with Parkinson's disease, Parkinsonism & related disorders 19(1) (2013) 47-52.

[14] K. Varnas, Z. Cselenyi, A. Jucaite, C. Halldin, P. Svenningsson, L. Farde, A. Varrone, PET imaging of [(11)C]PBR28 in Parkinson's disease patients does not indicate increased binding to TSPO despite reduced dopamine transporter binding, European journal of nuclear medicine and molecular imaging 46(2) (2019) 367-375.

[15] D.R. Owen, A.J. Yeo, R.N. Gunn, K. Song, G. Wadsworth, A. Lewis, C. Rhodes, D.J. Pulford, I. Bennacef, C.A. Parker, P.L. StJean, L.R. Cardon, V.E. Mooser, P.M. Matthews, E.A. Rabiner, J.P. Rubio, An 18-kDa translocator protein (TSPO) polymorphism explains differences in binding affinity of the PET radioligand PBR28, Journal of cerebral blood flow and metabolism : official journal of the International Society of Cerebral Blood Flow and Metabolism 32(1) (2012) 1-5.

[16] T. Terada, M. Yokokura, E. Yoshikawa, M. Futatsubashi, S. Kono, T. Konishi, H. Miyajima, T. Hashizume, Y. Ouchi, Extrastriatal spreading of microglial activation in Parkinson's disease: a positron emission tomography study, Annals of nuclear medicine 30(8) (2016) 579-87.

[17] S. Lavisse, D. Garcia-Lorenzo, M.A. Peyronneau, B. Bodini, C. Thiriez, B. Kuhnast, C. Comtat, P. Remy, B. Stankoff, M. Bottlaender, Optimized Quantification of Translocator Protein Radioligand (1)(8)F-DPA-714 Uptake in the Brain of Genotyped Healthy Volunteers, J Nucl Med 56(7) (2015) 1048-54.

[18] D. Garcia-Lorenzo, S. Lavisse, C. Leroy, C. Wimberley, B. Bodini, P. Remy, M. Veronese, F. Turkheimer, B. Stankoff, M. Bottlaender, Validation of an automatic reference region extraction

for the quantification of [(18)F]DPA-714 in dynamic brain PET studies, Journal of cerebral blood flow and metabolism : official journal of the International Society of Cerebral Blood Flow and Metabolism 38(2) (2018) 333-346.
[19] B. Kuhnast, A. Damont, F. Hinnen, T. Catarina, S. Demphel, S. Le Helleix, C. Coulon, S. Goutal, P. Gervais, F. Dolle, [18F]DPA-714, [18F]PBR111 and [18F]FEDAA1106-selective radioligands for imaging TSPO 18 kDa with PET: automated radiosynthesis on a TRACERLAb FX-FN synthesizer and quality controls, Applied radiation and isotopes : including data, instrumentation and methods for use in agriculture, industry and medicine 70(3) (2012) 489-97.
[20] D. Guilloteau, P. Emond, J.L. Baulieu, L. Garreau, Y. Frangin, L. Pourcelot, L. Mauclaire, J.C. Besnard, S. Chalon, Exploration of the dopamine transporter: in vitro and in vivo characterization of a high-affinity and high-specificity iodinated tropane derivative (E)-N-(3-iodoprop-2-enyl)-2beta-carbomethoxy-3beta-(4'-m ethylph enyl)nortropane (PE2I), Nuclear medicine and biology 25(4) (1998) 331-7.
[21] F.C. Sureau, A.J. Reader, C. Comtat, C. Leroy, M.J. Ribeiro, I. Buvat, R. Trebossen, Impact of image-space resolution modeling for studies with the high-resolution research tomograph, J Nucl Med 49(6) (2008) 1000-8.
[22] J.V. Manjon, P. Coupe, volBrain: An Online MRI Brain Volumetry System, Front Neuroinform 10 (2016) 30.
[23] M. Schain, K. Varnas, Z. Cselenyi, C. Halldin, L. Farde, A. Varrone, Evaluation of two automated methods for PET region of interest analysis, Neuroinformatics 12(4) (2014) 551-62.
[24] J. Logan, Graphical analysis of PET data applied to reversible and irreversible tracers, Nuclear medicine and biology 27(7) (2000) 661-70.
[25] A. Jucaite, I. Odano, H. Olsson, S. Pauli, C. Halldin, L. Farde, Quantitative analyses of regional [11C]PE2I binding to the dopamine transporter in the human brain: a PET study, European journal of nuclear medicine and molecular imaging 33(6) (2006) 657-68.
[26] Y. Kang, P.D. Mozley, A. Verma, D. Schlyer, C. Henchcliffe, S.A. Gauthier, P.C. Chiao, B. He, A. Nikolopoulou, J. Logan, J.M. Sullivan, K.O. Pryor, J. Hesterman, P.J. Kothari, S. Vallabhajosula, Noninvasive PK11195-PET Image Analysis Techniques Can Detect Abnormal Cerebral Microglial Activation in Parkinson's Disease, J Neuroimaging 28(5) (2018) 496-505.
[27] C. Kobylecki, S.J. Counsell, N. Cabanel, T. Wachter, F.E. Turkheimer, K. Eggert, W. Oertel, D.J. Brooks, A. Gerhard, Diffusion-weighted imaging and its relationship to microglial activation in parkinsonian syndromes, Parkinsonism & related disorders 19(5) (2013) 527-32.
[28] P. Edison, I. Ahmed, Z. Fan, R. Hinz, G. Gelosa, K. Ray Chaudhuri, Z. Walker, F.E. Turkheimer, D.J. Brooks, Microglia, amyloid, and glucose metabolism in Parkinson's disease with and without dementia, Neuropsychopharmacology 38(6) (2013) 938-49.
[29] A.L. Bartels, A.T. Willemsen, J. Doorduin, E.F. de Vries, R.A. Dierckx, K.L. Leenders, [11C]-PK11195 PET: quantification of neuroinflammation and a monitor of anti-inflammatory treatment in Parkinson's disease?, Parkinsonism & related disorders 16(1) (2010) 57-9.
[30] Y. Ouchi, S. Yagi, M. Yokokura, M. Sakamoto, Neuroinflammation in the living brain of Parkinson's disease, Parkinsonism & related disorders 15 Suppl 3 (2009) S200-4.
[31] J. Blesa, I. Trigo-Damas, M. Dileone, N.L. Del Rey, L.F. Hernandez, J.A. Obeso, Compensatory mechanisms in Parkinson's disease: Circuits adaptations and role in disease modification, Exp Neurol 298(Pt B) (2017) 148-161.
[32] A. Gerhard, R.B. Banati, G.B. Goerres, A. Cagnin, R. Myers, R.N. Gunn, F. Turkheimer, C.D. Good, C.J. Mathias, N. Quinn, J. Schwarz, D.J. Brooks, [11C](R)-PK11195 PET imaging of microglial activation in multiple system atrophy, Neurology 61(5) (2003) 686-9.
[33] M.G. Stokholm, A. Iranzo, K. Ostergaard, M. Serradell, M. Otto, K.B. Svendsen, A. Garrido, D. Vilas, P. Borghammer, J. Santamaria, A. Moller, C. Gaig, D.J. Brooks, E. Tolosa, N. Pavese, Assessment of neuroinflammation in patients with idiopathic rapid-eye-movement sleep behaviour disorder: a case-control study, The Lancet. Neurology 16(10) (2017) 789-796.
[34] A.A. Roussakis, P. Piccini, Molecular Imaging of Neuroinflammation in Idiopathic Parkinson's Disease, Int Rev Neurobiol 141 (2018) 347-363.
[35] S. Venneti, B.J. Lopresti, C.A. Wiley, Molecular imaging of microglia/macrophages in the brain, Glia 61(1) (2013) 10-23.

FIGURE LEGENDS

Figure 1 : **A-**Midbrain regions of interest superimposed on an individual representative MRI; B-Representative merged [^{18}F]-DPA714 PET and MRI images at the midbrain level.

Legend: Scaling of the images is fixed for visual comparison. PET images are corrected for weight and injected dose and are normalized by the radioactivity value in the SVCA reference region (SUV_R). A mask of the midbrain has been applied on the PET image to show [^{18}F]-DPA714 activity in this region only. Normalized images are summed from 60 to 90 minutes. Middle: HAB HC and right: HAB PD patient. PET images are coregistered to the individual MRI.

Figure 2 : [^{18}F]-DPA714 BP_{ND} individual values in the putaminal and midbrain regions

*Legend: PD patients compared to HC bilaterally in the midbrain and in the putamen. + and – refer respectively to more and less affected sides in patients. BP_{ND} from left and right hemispheres are averaged in HC. * $p < 0.05$, ** $p < 0.01$ and *** $p < 0.001$, 2-way ANOVA followed by Tukey post hoc.*

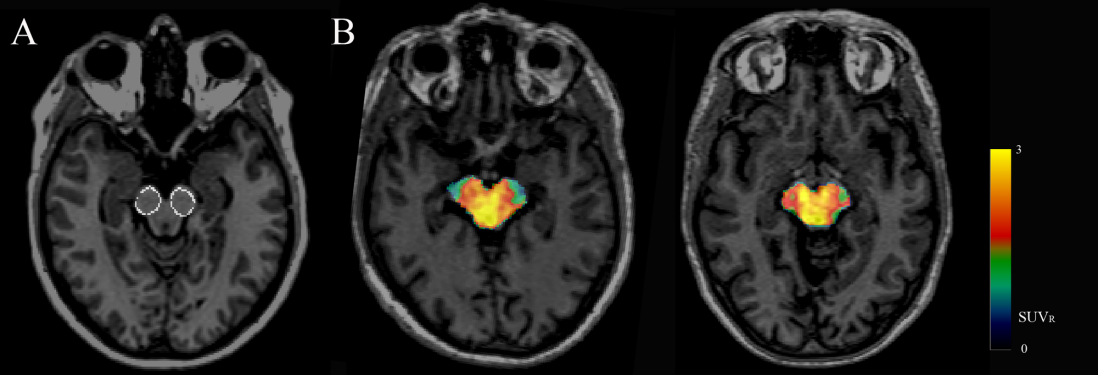
A
B
3
SUVR
0

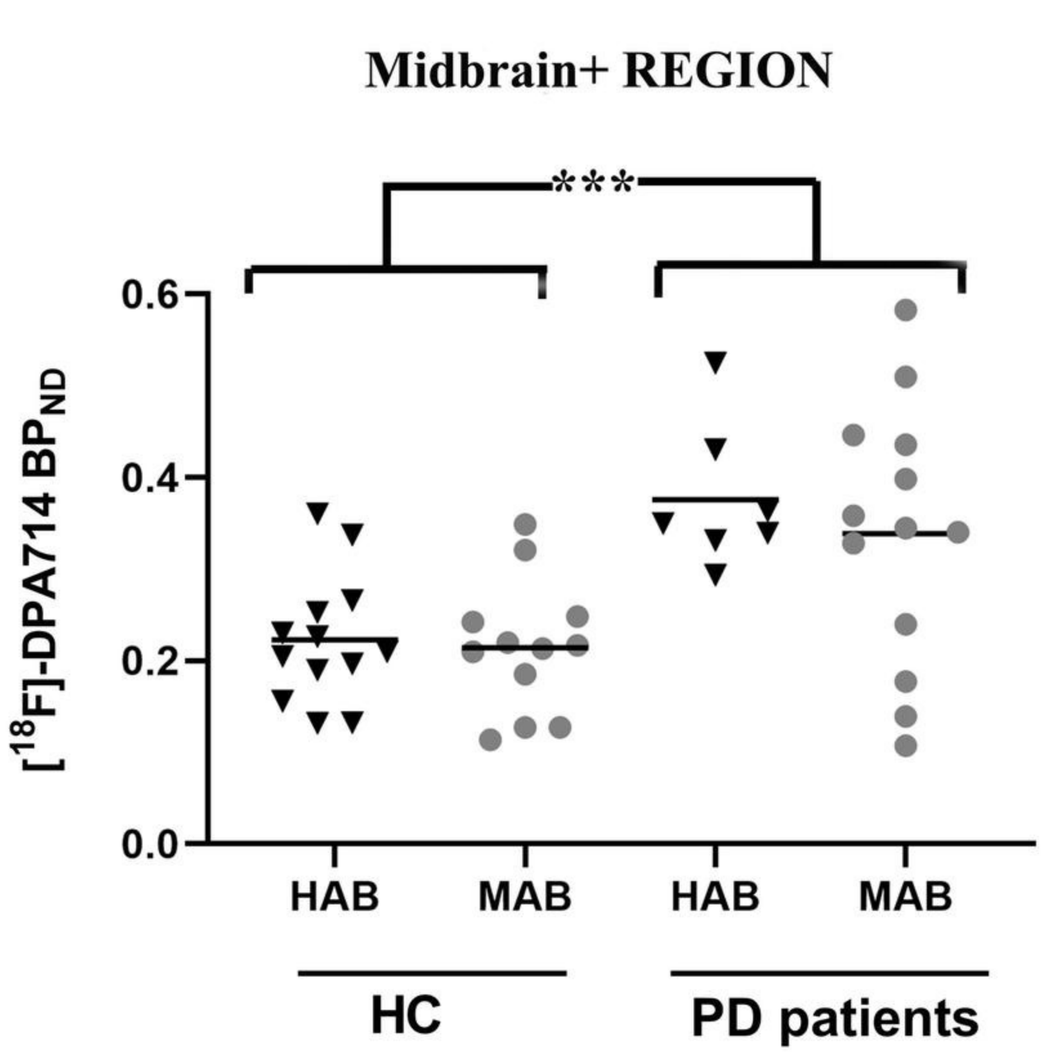
Midbrain+ REGION
***
[18F]-DPA714 BPND
0.6
0.4
0.2
0.0
HAB
MAB
HAB
MAB
HC
PD patients

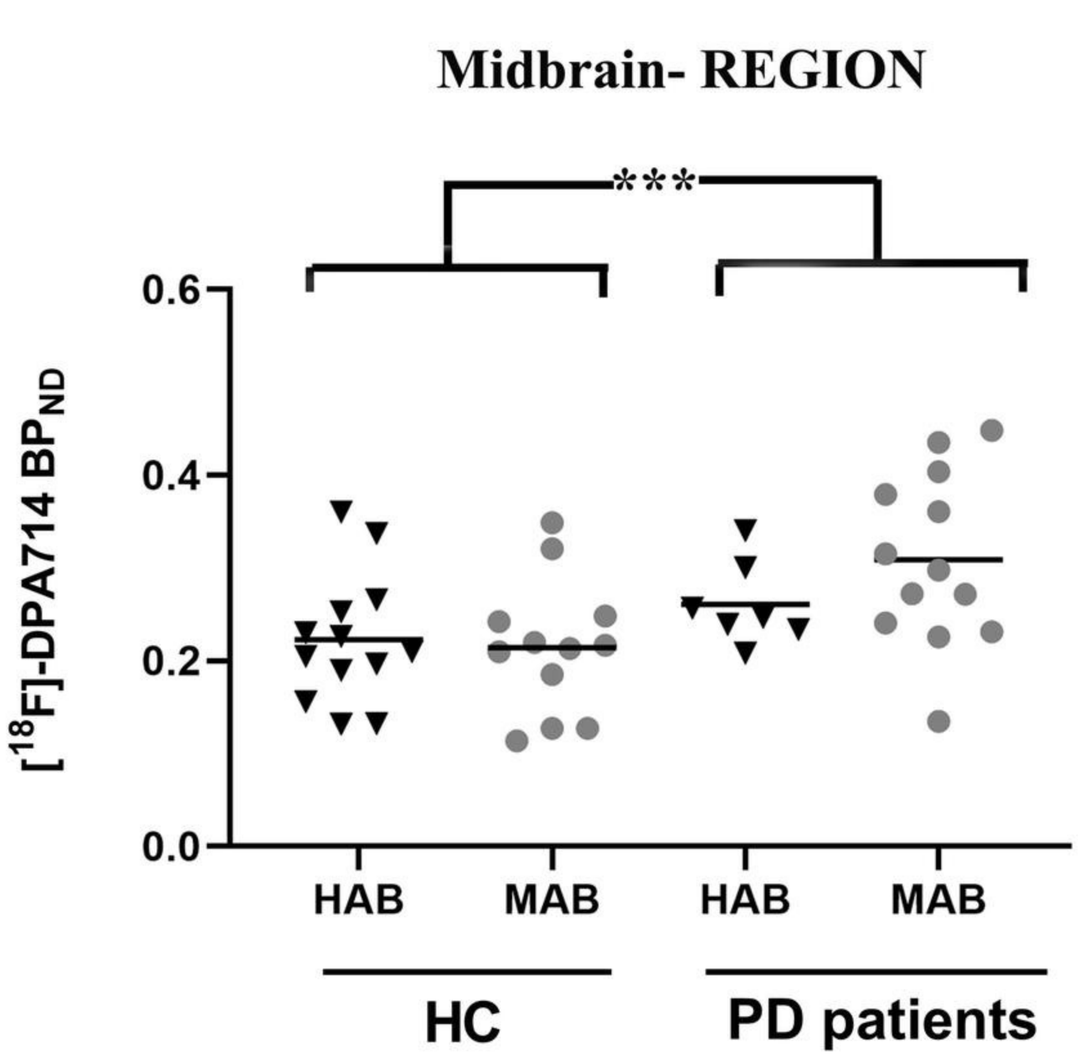
Midbrain- REGION
***
[18F]-DPA714 BPND
0.6
0.4
0.2
0.0
HAB
MAB
HAB
MAB
HC
PD patients

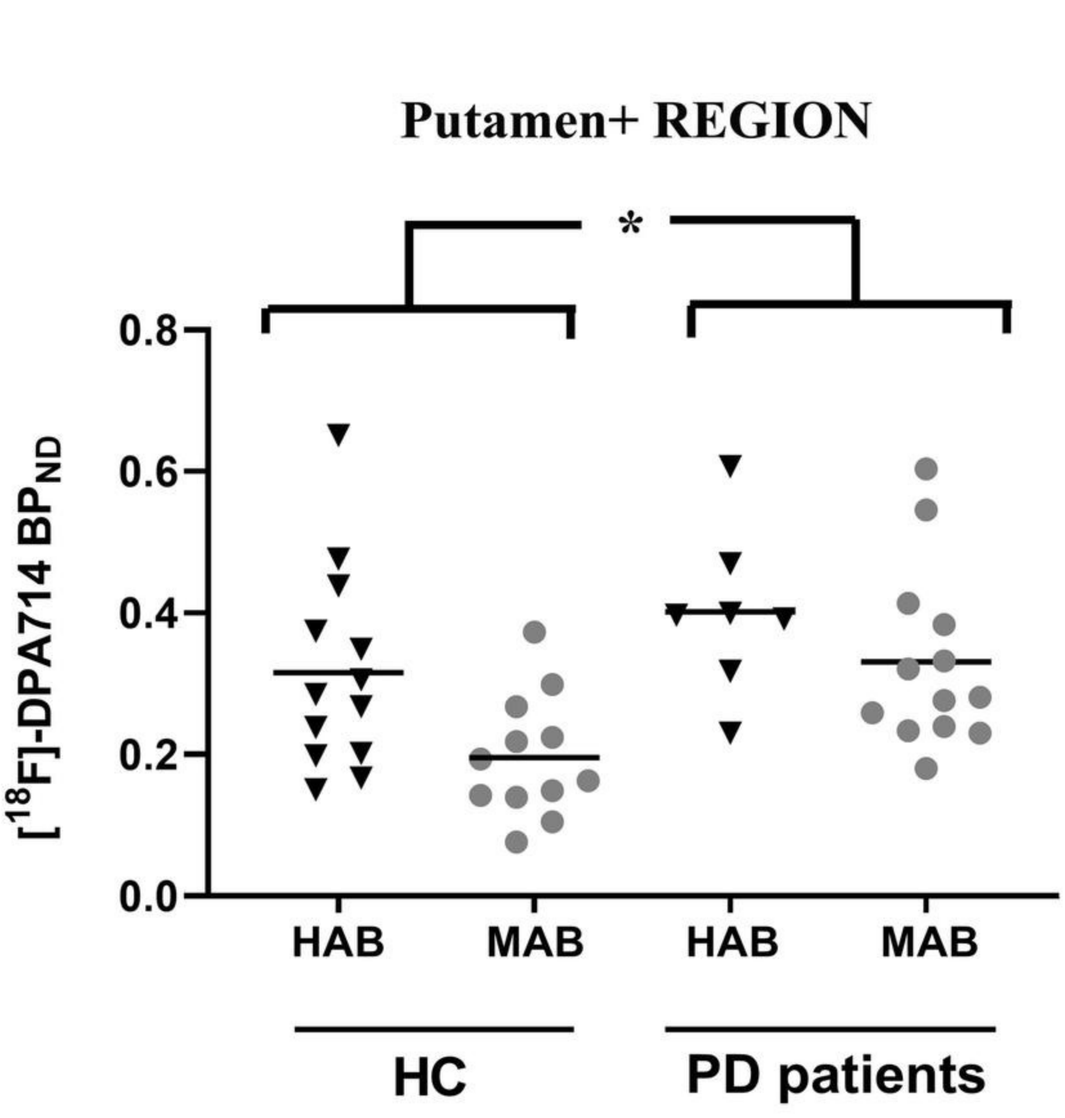
Putamen+ REGION
*
[18F]-DPA714 BPND
0.8
0.6
0.4
0.2
0.0
HAB
MAB
HAB
MAB
HC
PD patients

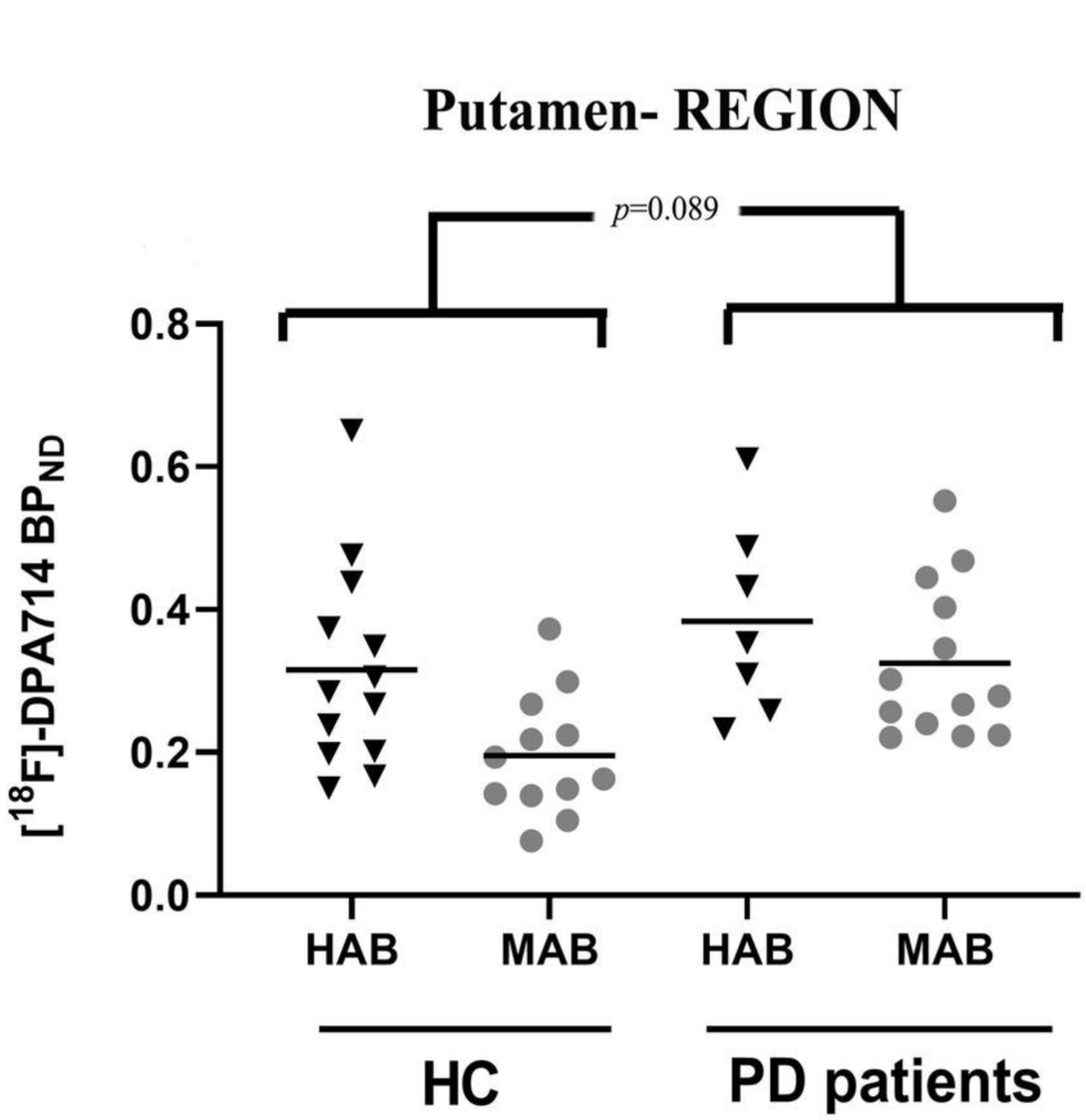
Putamen- REGION
p=0.089
[18F]-DPA714 BPND
0.8
0.6
0.4
0.2
0.0
HAB
MAB
HAB
MAB
HC
PD patients

Table 1 : Clinical characteristics of the Parkinson's disease patients.

Patients	Gender	Age	Genotype	Disease duration (mo)	UPDRS I	UPDRS II	UPDRS-III (off)	UPDRS IV	Hoehn et Yahr
1	F	63	MAB	30	0	7	6	0	2
2	M	58	HAB	36	0	0	12	0	2.5
3	M	57	MAB	30	1	5	13	0	2
4	F	52	MAB	1	1	2	13	0	1.5
5	M	69	MAB	1	0	1	14	0	1.5
6	M	55	HAB	18	1	4	14	0	1.5
7	F	72	LAB	30	1	4	17	0	2.5
8	F	63	MAB	60	1	4	19	0	1
9	M	46	HAB	18	2	6	19	0	2.5
10	M	66	MAB	120	1	8	19	5	2.5
11	F	78	MAB	6	4	8	19	0	2.5
12	M	80	na	2	0	4	13	0	1
13	M	59	LAB	5	1	5	20	0	3
14	M	60	HAB	36	0	4	21	0	2.5
15	M	76	LAB	156	2	8	21	6	3
16	F	66	MAB	13	4	22	23	1	1.5
17	M	78	MAB	1	2	14	23	0	2.5
18	M	71	HAB	108	2	7	24	6	3
19	M	66	HAB	72	4	16	25	4	2.5
20	M	72	MAB	6	3	5	26	0	2.5
21	M	66	HAB	132	13	16	27	8	2.5
22	M	63	MAB	30	1	6	28	0	2
23	F	67	MAB	60	0	7	29	1	2.5
24	F	58	MAB	108	1	2	34	3	3

<u>Legend</u>: HAB, MAB, LAB are respectively high affinity, mixed affinity and low affinity binders of [^{18}F]-DPA714. Disease duration is in months. MDS-UPDRS: Movement Disorder Society – Unified Parkinson Disease Rating Scale.

Table 2 : Regional microglial activation in HC and PD subjects : mean [^{18}F]-DPA-714 BP_{ND} and standard deviation values in different VOIs

	HC (BP_{ND}± SD)		**PD patients** (BP_{ND}± SD)		P-values - Diff PD/HC	P-values - TSPO polymorphism
	MAB	HAB	MAB	HAB		
Midbrain-	0.21±0.07	0.22±0.07	0.31± *0.09*	0.25± *0.09*	<0.001	NS
Midbrain+			0.34± *0.14*	0.37± *0.07*	<0.001	NS
Caudate -	-0.07±0.13	0.010±0.11	0.02± *0.146*	0.12± *0.161*	NS	NS
Caudate +			0.06± *0.191*	0.05± *0.283*	NS	NS
Putamen -	0.20±0.086	0.31±0.14	0.33± *0.109*	0.38± *0.135*	NS	0.045
Putamen +			0.33± *0.126*	0.40± *0.118*	0.038	0.016
Thal -	0.45±0.09	0.58±0.08	0.50± *0.144*	0.60± *0.090*	NS	0.006
Thal +			0.43± *0.176*	0.57± *0.131*	NS	<0.001
GP -	0.20±0.07	0.32±0.09	0.24± *0.086*	0.32± *0.089*	NS	<0.001
GP +			0.26± *0.096*	0.40± *0.167*	NS	<0.001
Occipital	0.30± *0.11*	0.35± *0.15*	0.35± *0.091*	0.34± *0.10*	NS	NS
Frontal	0.42 ± *0.10*	0.53 ± *0.42*	0.60 ± *0.17*	0.71 ± *0.20*	0.001	NS
Parietal	0.32 ± *0.18*	0.41 ± *0.15*	0.40 ± *0.13*	0.46± *0.17*	NS	NS
Temporal	0.20 ± *0.038*	0.25 ± *0.071*	0.24± *0.05*	0.26± *0.12*	NS	NS

Legend : Regional mean binding potential values (BP_{ND}) for all subjects. + and - refer respectively to the most and less affected sides in patients. Left and right hemispheres are averaged for cortical regions. SD = standard deviation. Statistical differences between HC (healthy controls) and patients (HABs+MABs) are provided as p-values in the third column when significant (two-ways ANOVA). Last column: statistical impact of the TSPO polymorphism on the HC and PD patients difference. NS = non significant